

Impact of ordering competition on the global phase diagram of iron pnictides

Jing Wang and Guo-Zhu Liu

Department of Modern Physics, University of Science and Technology of China, Hefei, Anhui 230026, P.R. China

We consider the impact of the competition among superconductivity, spin density wave, and nematic order in iron pnictides, and show that the ordering competition substantially reshapes the global phase diagram. We perform a detailed renormalization group analysis of an effective field theory of iron pnictides and derive the flow equations of all the physical parameters. Using these results, we find that superconductivity can be strongly suppressed by the ordering competition, and also extract the T -dependence of superfluid density. Moreover, the phase transitions may become first order. Interestingly, our RG analysis reveal that the nematic order exists only in an intermediate temperature region $T_m < T < T_n$, but is destroyed at $T > T_n$ by thermal fluctuation and at $T < T_m$ by ordering competition. This anomalous existence of nematic order leads to a back-bending of the nematic transition line on the phase diagram, consistent with the observed reentrance of tetragonal structure at low temperatures. A modified phase diagram is obtained based on the RG results.

PACS numbers: 74.70.Xa, 74.20.Mn, 74.25.Ha, 74.40.Kb

Competition between distinct long-range orders is a common phenomenon that we frequently meet when studying a number of unconventional superconductors, including cuprates¹, heavy fermion compounds^{2,3}, and iron pnictides⁴⁻¹⁰. Although ordering competition is a general concept and occurs in various patterns, the most frequently studied is that superconductivity compete and coexist with antiferromagnetism or nematic order¹¹. When these orders coexist in a bulk superconductor, one expects that a well-defined quantum critical point (QCP) exists somewhere in the superconducting (SC) dome. An important question is how to probe the widely predicted QCP in realistic experiments.

Recently, we studied the physical effects of the competition between superconductivity and nematic order in a d -wave cuprate superconductor¹², and found that the superfluid density ρ_s is suppressed at the nematic QCP significantly. According to our analysis, the suppression of ρ_s is indeed caused by two scenarios. First, the ordering competition reduces the charge condensate. Second, the gapless nodal quasiparticles couple strongly to the critical fluctuation of nematic order, which excites more normal quasiparticles out of the condensate. We further showed that the suppression effect is significant solely at the QCP¹², thus ρ_s should exhibit a deep valley at this point. Based on these results, we proposed¹² that the nematic QCP can be probed by measuring London penetration depth λ_L , which satisfies $\lambda_L^{-2} \propto \rho_s$. Clearly, the deep valley of ρ_s corresponds to a sharp peak of λ_L .

Thus far, no experimental evidence for the suppression of superfluid density has been reported in cuprates. It is interesting that Hashimoto *et al.* have measured the penetration depth λ_L in an iron pnictide $\text{BaFe}_2(\text{As}_{1-x}\text{P}_x)_2$ and observed a sharp peak of λ_L ¹³, which was claimed to signal the existence of a QCP of certain competing order beneath the SC dome¹³. This observation has stimulated considerable theoretical interest¹⁴⁻¹⁶ on the properties of the proposed QCP in $\text{BaFe}_2(\text{As}_{1-x}\text{P}_x)_2$ and its relationship with the observed peak of λ_L .

However, the above finding seems to be at odds with

the fact that there are two transition lines going across the superconducting line T_c , namely a nematic transition line T_n and a spin density wave (SDW) transition line T_M . This important issue was addressed by Fernandes *et al.*¹⁶ within an effective theory that consists of SC, SDW, and nematic order parameters. The theoretical analysis of Ref.¹⁶ demonstrated that the SDW and nematic transition lines penetrate separately into the SC dome, but merge at certain temperature, giving rise to a single QCP, which is schematically shown in Fig. 1.

In spite of the interesting progress, our understanding of the physical effects of ordering competition is still quite limited, and more research effort is required. In particular, it is necessary to investigate how the global phase diagram is influenced by ordering competition, which can help us to clarify many important issues about the nature of quantum phase transitions in iron pnictides.

In this paper, we study the global phase diagram of some iron pnictides, such as $\text{BaFe}_2(\text{As}_{1-x}\text{P}_x)_2$ and $\text{Ba}(\text{Fe}_{1-x}\text{Co}_x)_2\text{As}_2$, by carefully investigating the impact of the competition among superconductivity, SDW order and nematic order. In order to examine the role played by the quantum fluctuation of various order parameters, we will perform an extensive renormalization group (RG) analysis^{17,18} and obtain the RG equations for all the physical parameters that are introduced to describe the system. We also extract the T -dependence of the superfluid density $\rho_s(T)$ from the solutions of RG equations, and find that the superconductivity may be drastically suppressed by the ordering competition. In addition, the RG results clearly show that the phase transitions become first order.

Moreover, we have paid special attention to the fate of the transition line of nematic order in the SC dome. Interestingly, our RG analysis have discovered that the nematic order can only exist in an intermediate temperature region $T_m < T < T_n$, but is destroyed at $T > T_n$ by thermal fluctuation and at $T < T_m$ by ordering competition. Such a phenomenon is found to occur in a wide region of the SC. This result indicates that the ne-

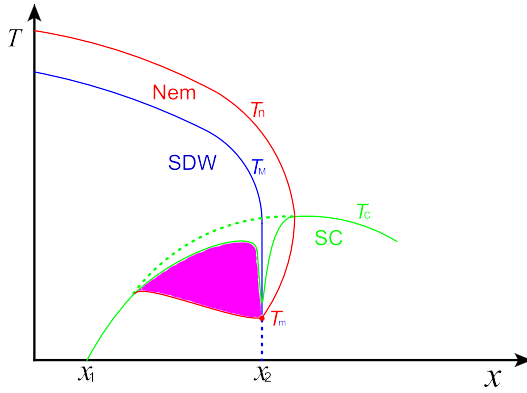


FIG. 1: Schematic phase diagram of iron pnictides on the $x - T$ plane^{16,19,20}, where x denotes the doping concentration. The two points x_1 and x_2 are the SC and SDW QCPs, respectively. The nematic transition line bends back towards lower x in the SC dome, showing reentrant behavior²¹.

magnetic transition line bends back towards lower values of x , which is shown in the schematic phase diagram Fig. 1. We notice that Nandi *et al.*²¹ have observed a reentrance of the tetragonal structure at low T in the SC dome. This observation is phenomenologically analogous to our theoretical result about the fate of nematic order.

It is known^{14,16} that many of the physical properties of $\text{BaFe}_2(\text{As}_{1-x}\text{P}_x)_2$ and $\text{Ba}(\text{Fe}_{1-x}\text{Co}_x)_2\text{As}_2$ can be described by a three-band model that composed of one hole pocket located at the center of the Brillouin zone $\mathbf{Q}_\Gamma = (0, 0)$ and two electron pockets centered at two specific momenta $\mathbf{Q}_X = (\pi, 0)$ and $\mathbf{Q}_Y = (0, \pi)$. The Hamiltonian is usually written as¹⁶

$$H = \sum_{\mathbf{k}, i \in (X, Y, \Gamma)} \varepsilon_{\mathbf{k}, i} c_{\mathbf{k}\sigma, i}^\dagger c_{\mathbf{k}\sigma, i} + H_4, \quad (1)$$

where H_4 represents two sorts of interactions:

$$H_4 = \sum_{\mathbf{k}, i \in (X, Y)} \frac{U_3}{2} \left(c_{\mathbf{k}\alpha, \Gamma}^\dagger c_{\mathbf{k}\gamma, \Gamma}^\dagger c_{\mathbf{k}\delta, i} c_{\mathbf{k}\beta, i} + \text{h.c.} \right) \delta_{\alpha\beta} \delta_{\gamma\delta} + \sum_{\mathbf{k}, i \in (X, Y)} U_1 c_{\mathbf{k}\alpha, \Gamma}^\dagger c_{\mathbf{k}\gamma, i}^\dagger c_{\mathbf{k}\delta, i} c_{\mathbf{k}\beta, \Gamma} \delta_{\alpha\beta} \delta_{\gamma\delta}. \quad (2)$$

Here, U_3 denotes the pair hopping interaction and U_1 the density-density interaction, which are responsible for the SDW order and superconductivity respectively^{16,22}. We mention here that the U_3 terms describe the magnetic Hund's coupling interactions^{23,24}, which are known to be important in multi-band electronic systems²⁵⁻²⁷. As demonstrated in Ref.¹⁶, the fermionic degrees of freedom can be fully integrated out, leading to

$$\begin{aligned} \mathcal{L} = & \frac{1}{2} (\partial_\mu M_X)^2 + \frac{1}{2} (\partial_\mu M_Y)^2 + a_m (M_X^2 + M_Y^2) \\ & + \frac{u_m}{2} (M_X^2 + M_Y^2)^2 - \frac{g_m}{2} (M_X^2 - M_Y^2)^2 \\ & + \partial_\mu \Delta^\dagger \partial_\mu \Delta + a_s \Delta^2 + \frac{u_s}{2} \Delta^4 \\ & + \zeta (M_X^2 + M_Y^2) \Delta^2, \end{aligned} \quad (3)$$

where the parameters a_m , a_s , u_s , u_m , g_m , and ζ are defined in¹⁶. This model will be our starting point. The transition lines for the SDW and SC orders are obtained by taking $a_m = 0$ and $a_s = 0$, respectively. $M_{X,Y}$ represent the SDW order parameters that generate long-range magnetic order for $(\pi, 0)$ and $(0, \pi)$ respectively^{16,28}. For s^{+-} -wave superconductor, a universal SC gap is introduced such that $\Delta_\Gamma = -\sqrt{2} \Delta_{X,Y} = \Delta^{16}$. An Ising-type nematic order is induced by the magnetic order²⁸, and represented by the $M_X^2 - M_Y^2$.

Fernandes *et al.*¹⁶ have recently studied the nature of quantum phase transitions in iron pnictides within the above effective theory and argued that the SDW and nematic orders merge at certain point in the SC dome. In this paper, we will make a systematic RG analysis. Our aim is two fold. First, we would like to examine the impact of the quantum fluctuations of SC and magnetic order parameters on the fate of phase transitions and the global phase diagram of the system, since these quantum fluctuations are known to play a vital role in systems that exhibit competing orders²⁹⁻³¹. Second, we attempt to extract the T -dependence of the superfluid density $\rho_s(T)$ from the RG solutions. As aforementioned, $\rho_s(T)$ can be suppressed by two different scenarios: the competitive interaction between distinct orders, and the coupling between fermionic quasiparticles and competing order. While the latter scenario has been studied in some recent references^{14,32}, the former is rarely considered in the literature¹². As will be shown below, the influence of ordering competition on $\rho_s(T)$ is prominent and can be efficiently obtained from our RG results.

To simplify consideration, we first concentrate on the SDW QCP, corresponding to x_2 on Fig. 1, at which $a_m = 0$ and the magnetic order parameters have vanishing mean values, i.e., $\langle M_X \rangle = \langle M_Y \rangle = 0$. In the SC dome, the SC order parameter develops a nonzero mean value, i.e., $\langle \Delta \rangle = V_0 = \sqrt{-a_s/u_s}$. To study the quantum fluctuation of Δ around $\langle \Delta \rangle$, we introduce two new fields h and η , and then decompose Δ as $\Delta = V_0 + \frac{1}{\sqrt{2}}(h + i\eta)$ with $\langle h \rangle = \langle \eta \rangle = 0$. Moreover, to compute the superfluid density, it is convenient to couple Δ to a gauge potential A . Recall that an important property of SC state is the happening of Anderson-Higgs mechanism, which leads to the Meissner effect. This mechanism needs to be properly included in the RG analysis. We now introduce gauge potential A to the effective theory via the standard minimal coupling, i.e., $\partial_\mu \Delta \rightarrow (\partial_\mu - i\zeta_{\Delta A} A_\mu) \Delta$, where $\zeta_{\Delta A}$ is the coupling between A and Δ . Straightforward calculations gives rise to the following effective model

$$\begin{aligned} \mathcal{L}_{\text{eff}} = & \frac{1}{2} (\partial_\mu M_X)^2 + \frac{1}{2} (\partial_\mu M_Y)^2 + \alpha_X M_X^2 + \alpha_Y M_Y^2 \\ & + \frac{\beta_X}{2} M_X^4 + \frac{\beta_Y}{2} M_Y^4 + \zeta_{XY} M_X^2 M_Y^2 \\ & + \frac{1}{2} (\partial_\mu h)^2 + \alpha_h h^2 + \frac{\beta_h}{2} h^4 + \gamma_h h^3 \\ & - \frac{1}{4} (\partial_\mu A_\nu - \partial_\nu A_\mu)^2 + \frac{\alpha_A}{2} A^2 \end{aligned}$$

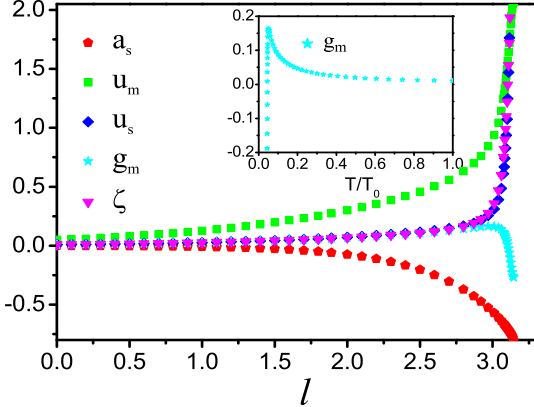


FIG. 2: Flows of a_s , u_m , u_s , g_m and ζ and T -dependence of g_m (inset) at SDW QCP. The parameter g_m is positive at small l and high T , but becomes negative suddenly once l exceeds some critical value l_m and T is lower than T_m .

$$+\gamma_{X^2h}M_X^2h + \gamma_{Y^2h}M_Y^2h + \zeta_{Xh}M_X^2h^2 \\ + \zeta_{Yh}M_Y^2h^2 + \gamma_{hA^2}hA^2 + \zeta_{hA}h^2A^2, \quad (4)$$

where we have defined a number of new effective parameters from a_m , a_s , u_s , u_m , g_m , ζ , and $\zeta_{\Delta A}$:

$$\alpha_X = \alpha_Y \equiv a_m - \frac{a_s \zeta}{u_s}, \beta_X = \beta_Y \equiv u_m - g_m, \\ \alpha_h \equiv -a_s, \beta_h \equiv \frac{u_s}{4}, \gamma_h \equiv \sqrt{\frac{-a_s u_s}{2}}, \alpha_A \equiv -\frac{2a_s \zeta_{\Delta A}}{u_s}, \\ \gamma_{hA^2} \equiv \zeta_{\Delta A} \sqrt{\frac{-2a_s}{u_s}}, \gamma_{X^2h} = \gamma_{Y^2h} \equiv \zeta \sqrt{\frac{-2a_s}{u_s}}, \\ \zeta_{XY} \equiv (u_m + g_m), \zeta_{Xh} = \zeta_{Yh} \equiv \frac{\zeta}{2}, \zeta_{hA} \equiv \frac{\zeta_{\Delta A}}{2}, \quad (5)$$

As a consequence of the Anderson-Higgs mechanism, the massless Goldstone boson induced by gauge symmetry breaking is swallowed by the gauge boson A , which then acquires an effective mass term $\frac{1}{2}\alpha_A A^2$. The superfluid density ρ_s is proportional to the gauge boson mass, i.e., $\rho_s \propto \alpha_A^{34}$. In the following, we will extract the T -dependence of $\rho_s(T)$ by computing the l -dependence of $\alpha_A \equiv \alpha_A(l)$, where l is a running length scale. However, α_A is related intimately to other parameters, so we need to solve all the RG equations self-consistently.

As shown in Eq. (5), all the new effective parameters are given by the seven original parameters. Our RG calculations are performed to the one-loop level in powers of the coupling constants. Analogous to the analysis of Ref.³¹, we have derived the RG equations for all the coupling parameters (See Supplemental Material³³ for the details).

To solve the equations, we assign the initial values of parameters as $a_s = -0.001$, $u_m = 0.05$, $u_s = 0.01$, $g_m = 0.01$, $\zeta = 0.01$, and $\zeta_{\Delta A} = 1.0 \times 10^{-8}$. SC and SDW orders are supposed to coexist, so u_s , u_m , g_m , and ζ satisfy the constraint $\zeta < \sqrt{u_s(u_m - g_m)}$ ^{16,35}. The main

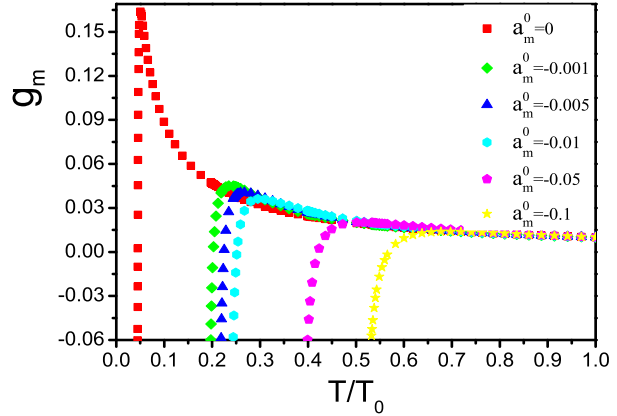


FIG. 3: T -dependence of g_m for different values of bare parameter a_m^0 , which measures the distance to SDW QCP x_2 . As a_m^0 grows, g_m varies with T similarly, but its peak disappears and the temperature for g_m to change sign increases.

conclusion is independent of these assumptions. There are three main results, to be explained one by one below.

First of all, we consider the fate of the associated phase transitions. After solving the RG equations, we show the l -dependence of various parameters in Fig. 2. The quadratic coupling parameters u_m , u_s , and ζ all flow to infinity eventually as $l \rightarrow +\infty$, thus the system does not approach any stable fixed point in the low energy region. As discussed in previous works^{29-31,36}, this results is usually regarded as a signature of an instability towards first-order transitions since a second-order transition is always associated with the presence of a stable infrared fixed point¹⁷. However, we can see from Fig. 2 that the parameters u_m , u_s , and ζ increase with growing l very slowly for small values of l . Their magnitudes become large only when l grows beyond certain threshold. Therefore, before running to large values, the RG results of the l -dependence of these parameters are still reliable and give us very useful information about the physical properties of the system³⁷.

Secondly, we address the impact of the ordering competition on the nematic transition line. A number of experiments have observed an interesting transition from an orthorhombic structure to a tetragonal structure at low T in the SC dome of $\text{Ba}(\text{Fe}_{1-x}\text{Co}_x)_2\text{As}_2$ ^{21,38,39} and $\text{Ba}(\text{Fe}_{1-x}\text{Rh}_x)_2\text{As}_2$ ⁴⁰. It turns out that the nematic order exists in an intermediate range of T and disappears once T is lower than certain value. Remarkably, this unusual behavior can be naturally obtained in our RG analysis. To demonstrate this, let us consider the property of parameter g_m , whose sign determines whether the nematic order is present. If $g_m > 0$, only one of the two order parameters M_X and M_Y develops a finite mean value^{20,28,41} due to tetragonal symmetry breaking. In this case, the nematic order is present. On the other hand, we have $\langle M_X \rangle = \langle M_Y \rangle$ if $g_m < 0$, which indicates that the nematic order is absent^{20,28,41}. Therefore, to judge whether

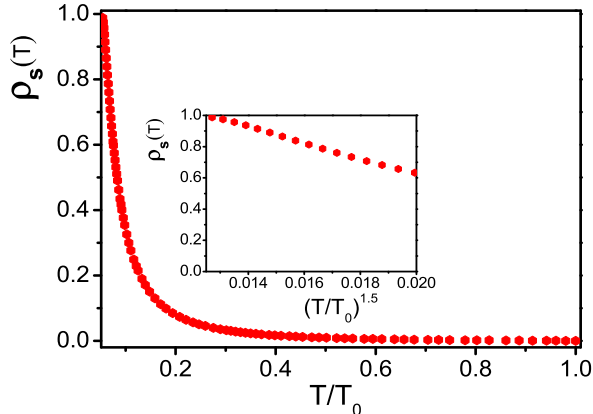


FIG. 4: Strong T -dependence of superfluid density $\rho_s(T)$ at the SDW QCP. The inset shows that $\rho_s(T)$ is similar to $(T/T_0)^{1.5}$ only in a very restricted temperature range.

the nematic order exists at certain T , we need to compute the T -dependence of g_m from the RG results.

The detailed l -dependence of g_m is depicted in Fig. 2. As l grows, g_m first increases steadily, but decreases rapidly for large values of l and becomes negative at certain critical value l_m . Notice that l_m is also the length scale at which u_m , u_s , and ζ diverge. We can translate the l -dependence of g_m to a T -dependence by using the transformation⁴² $T = T_0 e^{-l}$. The inset of Fig. 2 clearly shows that the positive g_m becomes negative as T decreases immediately below temperature $T_m = T_0 e^{-l_m}$, which means the nematic order is entirely suppressed at $T < T_m$. Therefore, the nematic order can only exist in the intermediate range between T_m and its transition temperature T_n . It is destroyed by the thermal fluctuation at $T > T_n$, and by the strong competition among superconductivity, SDW, and nematic order at $T < T_m$. Since T_n is supposed to be always higher than T_m ¹⁶, this behavior gives rise to a back-bending effect of the nematic transition line on the phase diagram shown in Fig. 1, which is consistent with the observed reentrance of tetragonal structure at low temperatures²¹.

To acquire a better knowledge of the phase diagram, we also wish to know how the nematic transition line varies with T as we move away from the SDW QCP. In the doping region $x_1 < x < x_2$, the SDW order parameters M_X and M_Y develop finite mean values. We here only present the main results (See Supplemental Material³³ for more details). Fig. 3 shows the T -dependence of g_m for different values of bare parameter a_m^0 . For the chosen values of a_m^0 , g_m always first grows with decreasing T and then becomes negative once T is below certain threshold, which means the nematic order is suppressed at low T . In addition, the temperature scale at which g_m changes sign increases as a_m^0 grows. In principle, the quantity T_0 , given by the SC transition temperature, also varies as a_m^0 grows. However, despite this complexity, one can conclude from our RG results that the nematic

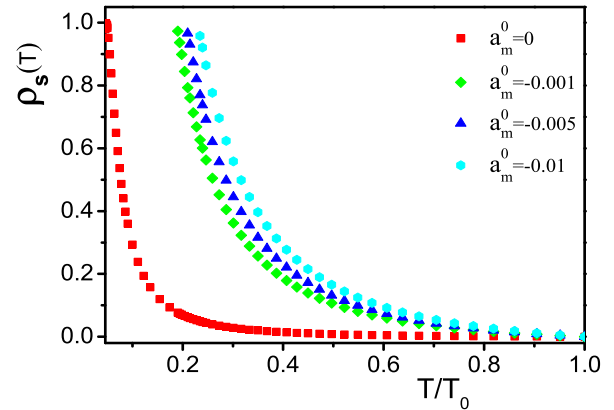


FIG. 5: $\rho_s(T)$ at different values of a_m^0 . The suppression of superfluid density takes place for any a_m^0 , but is most significant at the SDW QCP where $a_m^0 = 0$.

transition line cannot intersect with the horizontal axis of Fig. 1, but should instead merge somewhere with the SC transition line. This property leads to a considerable modification of the global phase diagram, as visualized in Fig. 1. According to our results, the reentrance of tetragonal phase occur in a wide range of doping x .

Finally, we turn to the T -dependence of superfluid density ρ_s . Within the effective model given by Eq. (4), the superfluid density $\rho_s \propto \alpha_A = -\frac{2a_s \zeta \Delta A}{u_s}$. To obtain the T -dependent $\lambda_L(T)$, we also utilize the transformation $T = T_0 e^{-l}$, where a suitable choice of T_0 is the SC temperature T_c . At first glance, the RG results seem to suggest that $\rho_s \propto \lambda_L^{-2}$ diverges rapidly at T_m . However, because the transitions become first order, the T -dependence of $\rho_s(T)$ is reliable only at $T > T_m$. Here, we choose the value $\rho_s(T^*)$ with T^* being a little higher than T_m to re-scale $\rho_s(T)$, and then show $\rho_s(T)/\rho(T^*)$ in Fig. 4, where the initial values are the same as those adopted in Fig. 2. An obvious conclusion is that the ordering competition leads to a strong T -dependence of ρ_s , which decreases very rapidly as T grows. For finite a_m^0 , the behaviors of $\rho_s(T)$ are depicted in Fig. 5. As a_m^0 increases, the suppression of $\rho_s(T)$ becomes weaker. Since T_c sensitively depends on the superfluid density, we can infer that T_c should be suppressed to some extent in the region $x_1 < x < x_2$ and that this effect is most significant at x_2 , as shown in Fig. 1.

Hashimoto *et al.*⁴³ has measured the superfluid density $\rho_s(T)$ in a number of superconductors, including iron pnictides and heavy fermion compounds, and claimed to unveil a universal $\rho_s(T) \propto T^{1.5}$ behavior over a wide range of temperatures. This behavior was argued^{32,43} to be caused by the coupling between magnetic fluctuation and fermionic excitations. Our analysis has clearly showed that ordering competition alone cannot account for the $\rho_s(T) \propto T^{1.5}$ behavior. As depicted in the inset of Fig. 4, only in a very restricted region of T could we extract an approximate $(T/T_0)^{1.5}$ behavior. On the other

hand, we can see from the main panel of Fig. 4 that, ordering competition does make a significant contribution to $\rho_s(T)$ and hence cannot be simply neglected. Bearing these two points in mind, we believe that both ordering competition and fermionic excitations need to be properly incorporated in a more refined model of $\rho_s(T)$.

In summary, we have studied the impact of the strong competition among superconductivity, SDW order, and nematic order on the global phase diagram of iron pnictides by performing a systematic RG analysis within an

effective field theory. The main results are summarized in the schematic phase diagram presented in Fig. 1.

J.W. is supported by the China Postdoctoral Science Foundation under Grants 2015T80655 and 2014M560510, the National Natural Science Foundation of China under Grant 11504360 and the Fundamental Research Funds for the Central Universities (P. R. China) under Grant WK2030040074. G.Z.L. is supported by the National Natural Science Foundation of China under Grant 11274286.

¹ P. A. Lee, N. Nagaosa, and X.-G. Wen, Rev. Mod. Phys. **78**, 17 (2006).

² H. v. Löhneysen, A. Rosch, M. Vojta, and P. Wölfle, Rev. Mod. Phys. **79**, 1015 (2007).

³ O. Stockert, S. Kirchner, F. Steglich, and Q. Si, J. Phys. Soc. Jpn. **81**, 011001 (2012).

⁴ Y. Kamihara, T. Watanabe, M. Hirano, H. Hosono, J. Am. Chem. Soc. **130**, 3296 (2008).

⁵ X. H. Chen, T. Wu, G. Wu, R. H. Liu, H. Chen, and D. F. Fang, Nature (London) **453**, 761 (2008).

⁶ G. F. Chen, Z. Li, D. Wu, G. Li, W. Z. Hu, J. Dong, P. Zheng, J. L. Luo, and N. L. Wang, Phys. Rev. Lett. **100**, 247002 (2008).

⁷ M. Rotter, M. Tegel, and D. Johrendt, Phys. Rev. Lett. **101**, 107006 (2008).

⁸ I. R. Fisher, L. Degiorgi, and Z. X. Shen, Rep. Prog. Phys. **74**, 124506 (2011).

⁹ P. J. Hirschfeld, M. M. Korshunov, and I. I. Mazin, Rep. Prog. Phys. **74**, 124508 (2011).

¹⁰ A. V. Chubukov, Annu. Rev. Condens. Matter Phys. **3**, 57 (2012).

¹¹ M. Vojta, Adv. Phys. **58**, 699 (2009); E. Fradkin *et al.*, Annu. Rev. Condens. Matter Phys. **1**, 153 (2010).

¹² G.-Z. Liu, J.-R. Wang, and J. Wang, Phys. Rev. B **85**, 174525 (2012).

¹³ K. Hashimoto, K. Cho, T. Shibauchi, S. Kasahara, Y. Mizukami, R. Katsumata, Y. Tsuruhara, T. Terashima, H. Ikeda, M.A. Tanatar, H. Kitano, N. Salovich, R.W. Giannetta, P. Walmsley, A. Carrington, R. Prozorov, and Y. Matsuda, Science **336**, 1554 (2012).

¹⁴ A. Levchenko, M. G. Vavilov, M. Khodas, and A.V. Chubukov, Phys. Rev. Lett. **111**, 177003 (2013).

¹⁵ D. Chowdhury, B. Swingle, E. Berg, and S. Sachdev, Phys. Rev. Lett. **111**, 157004 (2013).

¹⁶ R. M. Fernandes, S. Maiti, P. Wölfle, and A. V. Chubukov, Phys. Rev. Lett. **111**, 057001 (2013).

¹⁷ K. G. Wilson, Rev. Mod. Phys. **47**, 773 (1975).

¹⁸ R. Shankar, Rev. Mod. Phys. **66**, 129 (1994).

¹⁹ E. G. Moon and S. Sachdev, Phys. Rev. B **82**, 104516 (2010).

²⁰ R. M. Fernandes, A. V. Chubukov, and J. Schmalian, Nat. Phys. **10**, 97 (2014).

²¹ S. Nandi, M. G. Kim, A. Kreyssig, R. M. Fernandes, D. K. Pratt, A. Thaler, N. Ni, S. L. Bud'ko, P. C. Canfield, J. Schmalian, R. J. McQueeney, and A. I. Goldman, Phys. Rev. Lett. **104**, 057006 (2010).

²² S. Maiti and A. V. Chubukov, Phys. Rev. B **82**, 214515 (2010).

²³ A. V. Chubukov, D. V. Efremov, and I. Eremin, Phys. Rev. B **78**, 134512 (2008).

²⁴ F. Wang, H. Zhai, Y. Ran, A. Vishwanath, D.-H. Lee Phys. Rev. Lett. **102**, 047005 (2009).

²⁵ L. de' Medici, Phys. Rev. B **83**, 205112 (2011).

²⁶ T. Schickling, F. Gebhard, J. Büinemannand, L. Boeri, O. K. Andersen, and W. Weber, Phys. Rev. Lett. **108**, 036406 (2012).

²⁷ L. de' Medici, G. Giovannetti, and M. Capone, Phys. Rev. Lett. **112**, 177001 (2014).

²⁸ R. M. Fernandes, A. V. Chubukov, J. Knolle, I. Eremin, and J. Schmalian, Phys. Rev. B **85**, 024534 (2012).

²⁹ J.-H. She, J. Zaanen, A. R. Bishop, and A. V. Balatsky, Phys. Rev. B **82**, 165128 (2010).

³⁰ Z. Nussinov, I. Vekhter and A. V. Balatsky, Phys. Rev. B **79**, 165122 (2009); A. J. Millis, Phys. Rev. B **81**, 035117 (2010).

³¹ J. Wang and G.-Z. Liu, Phys. Rev. D **90**, 125015 (2014).

³² T. Nomoto and H. Ikeda, Phys. Rev. Lett. **111**, 167001 (2013).

³³ See Supplemental Material at <http://> for more detailed analytical treatment of the effective theory and for the expression of the coupled RG equations of all the effective parameters.

³⁴ B. I. Halperin, T. C. Lubensky, and S.-K. Ma, Phys. Rev. Lett. **32**, 292 (1974).

³⁵ R. M. Fernandes and J. Schmalian, Phys. Rev. B **82**, 014521 (2010).

³⁶ E. Domany, D. Mukamel, and M. E. Fisher, Phys. Rev. B **15**, 5432 (1977); J. H. Chen, T. C. Lubensky, and D. R. Nelson, Phys. Rev. B **17**, 4274 (1978); J. Rudnick, Phys. Rev. B **18**, 1406 (1978); H. H. Iacobson and D. J. Amit, Ann. Phys. **133**, 57 (1981).

³⁷ J. Wang, A. Eberlein, and W. Metzner, Phys. Rev. B **89**, 121116(R) (2014).

³⁸ D. K. Pratt, W. Tian, A. Kreyssig, J. L. Zarestky, S. Nandi, N. Ni, S. L. Bud'ko, P. C. Canfield, A. I. Goldman, and R. J. McQueeney, Phys. Rev. Lett. **103**, 087001 (2009).

³⁹ A. D. Christianson, M. D. Lumsden, S. E. Nagler, G. J. MacDougall, M. A. McGuire, A. S. Sefat, R. Jin, B. C. Sales, and D. Mandrus, Phys. Rev. Lett. **103**, 087002 (2009).

⁴⁰ A. Kreyssig, M. G. Kim, S. Nandi, D. K. Pratt, W. Tian, J. L. Zarestky, N. Ni, A. Thaler, S. L. Bud'ko, P. C. Canfield, R. J. McQueeney, and A. I. Goldman, Phys. Rev. B **81**, 134512 (2010).

⁴¹ R. M. Fernandes, S. A. Kivelson, and E. Berg,

arXiv:1504.03656.

⁴² J.-H. She, M. J. Lawler, and E.-A. Kim, Phys. Rev. B **92**, 035112 (2015).

⁴³ K. Hashimoto, Y. Mizukami, R. Katsumata, H. Shishido, M. Yamashita, H. Ikeda, Y. Matsuda, J. A. Schlueter, J. D. Fletcher, A. Carrington, D. Gnida, D. Kaczorowski, and T. Shibauchi, PNAS **110**, 3293 (2013).

I. SUPPLEMENTARY MATERIAL: IMPACT OF ORDERING COMPETITION ON THE GLOBAL PHASE DIAGRAM OF IRON PNICTIDES

The 122-family iron-based superconductors, such as $\text{BaFe}_2(\text{As}_{1-x}\text{P}_x)_2$ and $\text{Ba}(\text{Fe}_{1-x}\text{Co}_x)_2\text{As}_2$ are widely described in the literature^{14,16} by a three-band model that is composed of one hole pocket located at the center of the Brillouin zone $\mathbf{Q}_\Gamma = (0, 0)$ and two electron pockets centered at two specific momenta $\mathbf{Q}_X = (\pi, 0)$ and $\mathbf{Q}_Y = (0, \pi)$. Recently, this model was used by Fernandes *et al.* to study the nature of quantum phase transitions in the superconducting dome of some iron pnictides¹⁶. After integrating out the fermionic degrees of freedom¹⁶ and including the kinetic terms, one can obtain an effective Lagrangian density

$$\mathcal{L} = \frac{1}{2}(\partial_\mu M_X)^2 + \frac{1}{2}(\partial_\mu M_Y)^2 + a_m(M_X^2 + M_Y^2) + \frac{u_m}{2}(M_X^2 + M_Y^2)^2 - \frac{g_m}{2}(M_X^2 - M_Y^2)^2 + \partial_\mu \Delta^\dagger \partial_\mu \Delta + a_s \Delta^2 + \frac{u_s}{2} \Delta^4 + \zeta(M_X^2 + M_Y^2) \Delta^2, \quad (6)$$

where the parameters a_m , a_s , u_s , u_m , g_m , and ζ , are defined in Ref.¹⁶. Our RG analysis starts from this effective field theory. In order to examine the effect of ordering competition on the superfluid density, we introduce a small external gauge potential A that couples to the superconducting order parameter³⁴ and thus have an additional term

$$\mathcal{L}' = -\frac{1}{4}(\partial_\mu A_\nu - \partial_\nu A_\mu)^2 + \zeta_{\Delta A} |\Delta|^2 A^2, \quad (7)$$

where the Lorentz gauge $\partial_\mu A_\mu = 0$ is utilized and the parameter $\zeta_{\Delta A}$ is a new coupling constant.

In the superconducting dome, the order parameter Δ acquires a finite vacuum expectation value, i.e.,

$$V_0 \equiv \langle \Delta \rangle = \sqrt{\frac{-a_s}{u_s}}. \quad (8)$$

The quantum fluctuation of Δ around its mean value is believed to play an important role³¹ and needs to be seriously taken into account. It is convenient to introduce two new fields h and η by defining

$$\Delta = V_0 + \frac{1}{\sqrt{2}}(h + i\eta), \quad (9)$$

with $\langle h \rangle = \langle \eta \rangle = 0$. In many field-theoretic treatments of ordering competition, specially in the context of condensed matter systems, the quantum fluctuation of order parameter in the ordered phase is usually omitted. However, more careful analysis³¹ have showed that this approximation is not appropriate and that the order parameter fluctuation around its mean value can be significant. In order to entirely reveal the physical effects of ordering competition, we will consider h and η as quantum field operators and study their interactions with the magnetic order parameters M_X and M_Y .

Substituting the re-parameterized field operator Eq. (9) into the total Lagrangian density, we get a new effective model

$$\begin{aligned} \mathcal{L}_{\text{eff}} = & \frac{1}{2}(\partial_\mu M_X)^2 + \frac{1}{2}(\partial_\mu M_Y)^2 + \alpha_X M_X^2 + \alpha_Y M_Y^2 + \frac{\beta_X}{2} M_X^4 + \frac{\beta_Y}{2} M_Y^4 + \zeta_{XY} M_X^2 M_Y^2 \\ & + \frac{1}{2}(\partial_\mu h)^2 + \alpha_h h^2 + \frac{\beta_h}{2} h^4 + \gamma_h h^3 - \frac{1}{4}(\partial_\mu A_\nu - \partial_\nu A_\mu)^2 + \frac{\alpha_A}{2} A^2 + \gamma_{X^2 h} M_X^2 h \\ & + \gamma_{Y^2 h} M_Y^2 h + \zeta_{Xh} M_X^2 h^2 + \zeta_{Yh} M_Y^2 h^2 + \gamma_{hA^2} h A^2 + \zeta_{hA} h^2 A^2, \end{aligned} \quad (10)$$

where a number of effective parameters are defined on the basis of the fundamental parameters a_m , a_s , u_s , u_m , g_m , ζ , and $\zeta_{\Delta A}$, as given by Eq. (5) in the main part of the paper. Our RG analysis will be based on this effective model, assuming that the coupling constants take small values.

We now proceed to treat the effective theory by performing a detailed RG analysis¹⁸. To this end, we first make the following scaling transformations

$$k_i = k'_i e^{-l},$$

$$\begin{aligned}\omega &= \omega' e^{-l}, \\ q_i &= q'_i e^{-l}, \\ \epsilon &= \epsilon' e^{-l},\end{aligned}\tag{11}$$

where $i = x, y$ and l is a running length scale. Under these transformations, the field operators M_X , M_Y , h , and η should be re-scaled as

$$\begin{aligned}M_X(\mathbf{k}, \omega) &= M'_X(\mathbf{k}', \omega') e^{5l/2}, \\ M_Y(\mathbf{k}, \omega) &= M'_Y(\mathbf{k}', \omega') e^{5l/2}, \\ h(\mathbf{k}, \omega) &= h'(\mathbf{k}', \omega') e^{5l/2}, \\ A(\mathbf{q}, \epsilon) &= A'(\mathbf{q}', \epsilon') e^{5l/2}.\end{aligned}\tag{12}$$

In order to obtain the flow equations of the fundamental parameters defined in Eq. (6) and Eq. (7), we apply the following identities:

$$\begin{aligned}\frac{da_s}{dl} &= -\frac{d\alpha_h}{dl}, \\ \frac{du_s}{dl} &= 4\frac{d\beta_h}{dl}, \\ \frac{da_m}{dl} &= \frac{d\alpha_X}{dl} + \frac{\zeta}{u_s} \frac{da_s}{dl} + \frac{a_s}{u_s} \frac{d\zeta}{dl} - \frac{a_s \zeta}{u_s^2} \frac{du_s}{dl}, \\ \frac{du_m}{dl} &= \frac{1}{2} \frac{d\zeta_{XY}}{dl} + \frac{1}{2} \frac{d\beta_X}{dl}, \\ \frac{dg_m}{dl} &= \frac{1}{2} \frac{d\zeta_{XY}}{dl} - \frac{1}{2} \frac{d\beta_X}{dl}, \\ \frac{d\zeta}{dl} &= 2\frac{d\zeta_{Xh}}{dl}, \\ \frac{d\zeta_{\Delta A}}{dl} &= 2\frac{d\zeta_{hA}}{dl}.\end{aligned}\tag{13}$$

For simplicity, we first consider the SDW QCP with $a_m = 0$, where the magnetic order parameters M_X and M_Y both have vanishing mean values and their quantum fluctuations are critical. Analogous to the scheme presented in Ref.³¹, we have derived the following RG equations for the seven fundamental parameters

$$\begin{aligned}\frac{da_s}{dl} &= 2a_s - \frac{1}{12\pi^2} \left[\frac{27a_s u_s}{2} (1 + 4a_s) + \frac{12a_s \lambda^2}{u_s} \left(1 + \frac{4a_s \lambda}{u_s} \right) + 3\lambda \left(1 + \frac{2a_s \lambda}{u_s} \right) \right. \\ &\quad \left. + \frac{9u_s}{4} (1 + 2a_s) + 3\lambda_{\Delta A} \left(1 + \frac{2a_s \lambda_{\Delta A}}{u_s} \right) + \frac{32a_s \lambda_{\Delta A}^2}{u_s} \left(1 + \frac{4a_s \lambda_{\Delta A}}{u_s} \right) \right], \\ \frac{du_m}{dl} &= u_m + \frac{1}{2\pi^2} \left\{ (8u_m g_m - 17u_m^2 - 11g_m^2) \left(\frac{4a_s \lambda}{u_s} + 1 \right) - \frac{3\lambda^2}{8} (4a_s + 1) \right. \\ &\quad \left. + \frac{16a_s \lambda^2}{u_s} (2u_m - g_m) \left(1 + \frac{4a_s \lambda}{u_s} + 2a_s \right) - \frac{6a_s \lambda^3}{u_s} \left[1 + 2 \left(\frac{a_s \lambda}{u_s} + 2a_s \right) \right] \right\}, \\ \frac{du_s}{dl} &= u_s + \frac{1}{\pi^2} \left\{ 2\lambda^2 \left[4 \left(a_m - \frac{a_s \lambda}{u_s} \right) - 1 \right] - \frac{9u_s^2}{4} (4a_s + 1) + 54a_s u_s^2 (1 + 6a_s) \right. \\ &\quad \left. - \frac{4\lambda_{\Delta A}^2}{3} \left(\frac{4a_s \lambda_{\Delta A}}{u_s} + 1 \right) + \frac{32a_s \lambda^3}{u_s} \left(1 + \frac{6a_s \lambda}{u_s} \right) + \frac{11072a_s \lambda_{\Delta A}^3}{35u_s} \left(1 + \frac{6a_s \lambda_{\Delta A}}{u_s} \right) \right\}, \\ \frac{dg_m}{dl} &= g_m + \frac{1}{2\pi^2} \left\{ 3(u_m^2 + 3g_m^2 - 8u_m g_m) \left(\frac{4a_s \lambda}{u_s} + 1 \right) + \frac{\lambda^2}{8} (4a_s + 1) \right. \\ &\quad \left. + \frac{16a_s \lambda^2}{u_s} (2g_m - u_m) \left(1 + \frac{4a_s \lambda}{u_s} + 2a_s \right) - \frac{2a_s \lambda^3}{u_s} \left[1 + 2 \left(\frac{a_s \lambda}{u_s} + 2a_s \right) \right] \right\}, \\ \frac{d\lambda}{dl} &= \lambda + \frac{1}{\pi^2} \left[\frac{4a_s \lambda^3}{u_s} \left(1 + \frac{4a_s \lambda}{u_s} + 2a_s \right) - \frac{3u_s \lambda}{8} (4a_s + 1) + 9a_s u_s \lambda (1 + 6a_s) - 2\lambda^2 \left(\frac{2a_s \lambda}{u_s} + 2a_s + 1 \right) \right. \\ &\quad \left. - \lambda (2u_m - g_m) \left(\frac{4a_s \lambda}{u_s} + 1 \right) + \frac{16a_s \lambda^2}{u_s} (2u_m - g_m) \left(1 + \frac{6a_s \lambda}{u_s} \right) + 6a_s \lambda^2 \left(1 + \frac{2a_s \lambda}{u_s} + 4a_s \right) \right], \\ \frac{d\lambda_{\Delta A}}{dl} &= \lambda_{\Delta A} + \frac{1}{3\pi^2} \left\{ 27a_s u_s \lambda_{\Delta A} (1 + 6a_s) - 12\lambda_{\Delta A}^2 \left(1 + 2a_s + \frac{2a_s \lambda_{\Delta A}}{u_s} \right) - \frac{9u_s \lambda_{\Delta A}}{8} (4a_s + 1) \right. \\ &\quad \left. + \frac{64a_s \lambda_{\Delta A}^3}{u_s} \left(1 + 2a_s + \frac{4a_s \lambda_{\Delta A}}{u_s} \right) + 36a_s \lambda_{\Delta A}^2 \left[1 + 2a_s \left(2 + \frac{\lambda_{\Delta A}}{u_s} \right) \right] \right\}.\end{aligned}\tag{14}$$

When the system moves away from the SDW QCP and goes to a lower doping concentration, the stripe-SDW order parameters M_X and M_Y also develop nonzero mean values, i.e.,

$$\langle M_X \rangle = \langle M_Y \rangle = \sqrt{-\frac{a_m}{2u_m}}.\tag{15}$$

To include the quantum fluctuation of M_X and M_Y around their mean values, we introduce two new fields ξ and χ :

$$M_X = \sqrt{-\frac{a_m}{2u_m}} + \xi, \quad (16)$$

$$M_Y = \sqrt{-\frac{a_m}{2u_m}} + \chi, \quad (17)$$

with $\langle \xi \rangle = \langle \chi \rangle = 0$. Now the problem becomes more complicated than the case of SDW QCP. After lengthy but straightforward calculations, we obtain a set of RG equations:

$$\begin{aligned} \frac{da_s}{dl} &= 2a_s - \frac{1}{4\pi^2} \left\{ \frac{18a_s u_s}{4} (1 + 4a_s) + \frac{4a_s \lambda^2}{u_s} \left[1 + 4 \left(\frac{a_s \lambda}{u_s} + a_m \right) \right] + \frac{32a_s \lambda^2 \Delta A}{3u_s} \left(1 + \frac{4\lambda \Delta A a_s}{u_s} \right) + \lambda \left[1 + 2 \left(\frac{a_s \lambda}{u_s} + a_m \right) \right] \right. \\ &\quad \left. + \frac{3u_s}{4} (1 + 2a_s) + \frac{8a_s a_m^2 \lambda^2}{u_s} \left[1 + 8 \left(\frac{a_s \lambda}{u_s} + a_m \right) \right] + \lambda \Delta A \left(1 + \frac{2\lambda \Delta A a_s}{u_s} \right) + 4a_m^2 \lambda \left[1 + 6 \left(\frac{a_s \lambda}{u_s} + a_m \right) \right] \right\}, \\ \frac{da_m}{dl} &= 2 \left(\frac{a_s \lambda}{u_s} + a_m \right) + \frac{1}{4\pi^2} \left\{ 12a_m \left[a_m (g_m + 5u_m) - 6u_m \right] \left[1 + 4 \left(\frac{a_s \lambda}{u_s} + a_m \right) \right] - 72a_m^3 u_m \left[1 + 8 \left(\frac{a_s \lambda}{u_s} + a_m \right) \right] \right. \\ &\quad \left. - \frac{4a_s \lambda^2}{u_s} \left[1 + 2 \left(\frac{a_s \lambda}{u_s} + a_m \right) + 2a_s \right] - 2(2u_m - g_m) \left[1 + 2 \left(\frac{a_s \lambda}{u_s} + a_m \right) \right] - \frac{\lambda}{2} (1 + 2a_s) \right. \\ &\quad \left. - 4a_m^2 (g_m - 17u_m) \left[1 + 6 \left(\frac{a_s \lambda}{u_s} + a_m \right) \right] \right\} + \left(\frac{\lambda}{u_s} \frac{da_s}{dl} + \frac{a_s}{u_s} \frac{d\lambda}{dl} - \frac{a_s \lambda}{u_s^2} \frac{du_s}{dl} \right), \\ \frac{du_m}{dl} &= u_m + \frac{1}{4\pi^2} \left\{ 576a_m u_m (2u_m - g_m) \left[1 + 6 \left(\frac{a_s \lambda}{u_s} + a_m \right) \right] - 16a_m^2 \left(130u_m^2 - 94u_m g_m + g_m^2 \right) \left[1 + 8 \left(\frac{a_s \lambda}{u_s} + a_m \right) \right] \right. \\ &\quad \left. + \frac{32a_s \lambda^2}{u_s} (2u_m - g_m) \left[(1 + 4a_m^2)(1 + 2a_s) + 4 \left(\frac{a_s \lambda}{u_s} + a_m \right) (1 + 8a_m^2) \right] + \frac{16a_s \lambda^3}{u_s} \left[1 + 2 \left(\frac{a_s \lambda}{u_s} + 2a_s \right) \right] \right. \\ &\quad \left. - (37u_m^2 + 25g_m^2 - 10u_m g_m) \left[1 + 4 \left(\frac{a_s \lambda}{u_s} + a_m \right) \right] + 4608a_m^3 u_m (2u_m - g_m) \left[1 + 10 \left(\frac{a_s \lambda}{u_s} + a_m \right) \right] \right\}, \\ \frac{dg_m}{dl} &= g_m + \frac{1}{2\pi^2} \left\{ \frac{32a_s \lambda^2}{u_s} (2g_m - u_m) \left[(1 + 4a_m^2)(1 + 2a_s) + 4 \left(\frac{a_s \lambda}{u_s} + a_m \right) (1 + 8a_m^2) \right] \right. \\ &\quad \left. - 4a_m^2 \left[(g_m + 73u_m)(7g_m - 5u_m) + 9(u_m - g_m)^2 \right] \left[1 + 8 \left(\frac{a_s \lambda}{u_s} + a_m \right) \right] \right. \\ &\quad \left. - \left[12(u_m - g_m)(2g_m - u_m) + 6(u_m + g_m)^2 - \frac{\lambda^2}{4} \right] \left[4 \left(\frac{a_s \lambda}{u_s} + a_m \right) + 1 \right] \right. \\ &\quad \left. + 576a_m u_m (2g_m - u_m) \left[6 \left(\frac{a_s \lambda}{u_s} + a_m \right) + 1 \right] \right\}, \\ \frac{du_s}{dl} &= u_s + \frac{4}{\pi^2} \left\{ \frac{27a_s u_s^2}{2} (1 + 6a_s) - \frac{144a_s a_m u_m \lambda^3}{u_s} \left[1 + 10 \left(\frac{a_s \lambda}{u_s} + a_m \right) \right] - \frac{\lambda^2}{2} \left[4 \left(\frac{a_s \lambda}{u_s} + a_m \right) + 1 \right] \right. \\ &\quad \left. - \frac{9u_s^2}{16} (4a_s + 1) - \frac{4\lambda^2 \Delta A}{3} \left(\frac{4\lambda \Delta A a_s}{u_s} + 1 \right) - a_m^2 \lambda^2 \left[1 + 8 \left(\frac{a_s \lambda}{u_s} + a_m \right) \right] \right. \\ &\quad \left. + \frac{8a_s \lambda^3}{u_s} \left(1 + \frac{6a_s \lambda}{u_s} \right) + \frac{2768a_s \lambda^3 \Delta A}{35u_s} \left(1 + \frac{6a_s \lambda \Delta A}{u_s} \right) \right\}, \\ \frac{d\lambda}{dl} &= \lambda + \frac{\lambda}{\pi^2} \left\{ 9a_s u_s (6a_s + 1) + 72a_m u_m \left[6 \left(\frac{a_s \lambda}{u_s} + a_m \right) + 1 \right] - (2u_m - g_m) \left[4 \left(\frac{a_s \lambda}{u_s} + a_m \right) + 1 \right] \right. \\ &\quad \left. - \frac{3u_s}{8} (4a_s + 1) + \frac{96a_s a_m^2 \lambda^2}{u_s} \left(\frac{a_s \lambda}{u_s} + a_m \right) - 2\lambda \left[1 - \frac{2a_s \lambda}{u_s} (1 + 4a_m^2) \right] \left[2a_s + 2 \left(\frac{a_s \lambda}{u_s} + a_m \right) + 1 \right] \right. \\ &\quad \left. - 4a_m^2 (20u_m - g_m) \left[1 + 8 \left(\frac{a_s \lambda}{u_s} + a_m \right) \right] + 576a_m^3 u_m \left(1 + 10 \left(\frac{a_s \lambda}{u_s} + a_m \right) \right) \right. \\ &\quad \left. + \frac{16a_s \lambda}{u_s} (2u_m - g_m) \left(1 + \frac{6a_s \lambda}{u_s} \right) + 6a_s \lambda \left[1 + 2a_s \left(\frac{\lambda}{u_s} + 2 \right) \right] \right\}, \\ \frac{d\lambda \Delta A}{dl} &= \lambda \Delta A + \frac{\lambda \Delta A}{3\pi^2} \left\{ 27a_s u_s (1 + 6a_s) - \frac{9u_s}{8} (4a_s + 1) + \frac{64a_s \lambda^2 \Delta A}{u_s} \left[1 + 2a_s \left(1 + \frac{2\lambda \Delta A}{u_s} \right) \right] \right. \\ &\quad \left. - 12\lambda \Delta A \left[1 + 2a_s \left(1 + \frac{\lambda \Delta A}{u_s} \right) \right] + 36a_s \lambda \Delta A \left[1 + 2a_s \left(2 + \frac{\lambda \Delta A}{u_s} \right) \right] \right\}. \end{aligned} \quad (18)$$

These equations are used to analyze the impact of ordering competition on the global phase diagram in the main context of the paper.